How to cite: Angew. Chem. Int. Ed. 2023, e202310978
doi.org/10.1002/anie.202310978

Dual Catalysis

Modular and Practical 1,2-Aryl(Alkenyl) Heteroatom Functionalization of Alkenes through Iron/Photoredox Dual Catalysis**

Weigang Zhang, Tao Liu, Hwee Ting Ang, Penghao Luo, Zhexuan Lei, Xiaohua Luo, Ming Joo Koh, and Jie Wu**

Abstract: Efficient methods for synthesizing 1,2-aryl-(alkenyl) heteroatomic cores, encompassing heteroatoms such as nitrogen, oxygen, sulfur, and halogens, are of significant importance in medicinal chemistry and pharmaceutical research. In this study, we present a mild, versatile and practical photoredox/iron dual catalytic system that enables access to highly privileged 1,2-aryl(alkenyl) heteroatomic pharmacophores with exceptional efficiency and site selectivity. Our approach exhibits an extensive scope, allowing for the direct utilization of a wide range of commodity or commercially available (hetero)arenes as well as activated and unactivated alkenes with diverse functional groups, drug scaffolds, and natural product motifs as substrates. By merging iron catalysis with the photoredox cycle, a vast array of alkene 1,2-aryl(alkenyl) functionalization products that incorporate a neighboring azido, amino, halo, thiocyano and nitrooxy group were secured. The scalability and ability to rapid synthesize numerous bioactive small molecules from readily available starting materials highlight the utility of this protocol.

Introduction

The rapid and efficient construction of molecular complexity from readily available starting materials has long been a fundamental pursuit in organic synthesis. In recent decades, transition-metal catalysis, photocatalysis, and electrosynthesis have emerged as powerful strategies for alkene difunctionalization, enabling the construction of two neighboring chemical bonds in a single transformation (Figure 1A,i).[1] Among these vicinal difunctionalizations, alkene 1,2-aryl heteroatom functionalization is of particular interest as it enables straightforward and step-economic synthesis of structurally diverse products by introducing a C–X bond (X = N, O, S, halogens, etc.) and a C–C(sp^2) bond simultaneously.[2] Furthermore, the incorporation of the 1,2-aryl heteroatomic motif has demonstrated enhancement in bio-efficacy and therapeutic potential, rendering it a privileged scaffold in pharmaceutical development[3] (Figure 1B). Although several transition-metal-catalyzed strategies for multicomponent 1,2-aryl heteroatom functionalization of alkenes have been developed, including carboboration,[4] arylhalogenation,[5] oxidative oxyarylation,[6] arylsulfenylation,[7] and the synthesis of cyclic arylethylamines,[8] most of these methods are limited by their narrow substrate scopes and the need for prefunctionalized starting materials, thus hindering their broad applicability.

Alternatively, radical-based intermolecular three-component approaches have emerged as a promising strategy for achieving alkene 1,2-aryl heteroatom functionalization (Figure 1A,ii). One of the classical methods is the Meerwein arylation that involves a reductive generation of aryl radicals from highly reactive precursors (aryldiazonium or diaryliodonium salts), followed by radical-polar crossover and trapping of the resulting carbocation with excess nucleophiles.[9] In 2021, the Gaunt group reported an excellent study on the vicinal azidoarylation of alkenes using diaryliodonium salts as aryl radical sources and NaN_3 as the heteroatom source, via a visible-light-mediated dual copper catalysis, to access β-aryl azidoalkanes.[10] However, the use of these reactive radical precursors presents challenges for the late-stage modification of complex bioactive molecules due to difficulties in accessing them. Conversely, readily available (hetero)arenes, which are prevalent in pharmaceutically relevant molecules, represent ideal aryl radical precursors (Figure 1C). However, generating aryl radicals through direct hydrogen atom abstraction of arenes is extremely challenging due to their high bond dissociation energy and site selectivity issues. To overcome this challenge, an elegant indirect approach using arylthianthrenium salts as aryl radical precursors was introduced by Ritter and co-workers in 2019,[11] and it has since been widely employed in two-component reactions.[12] The air and bench-stable arylthianthrenium salts can be derived from (hetero)arenes

[*] Dr. W. Zhang, T. Liu, Dr. H. T. Ang, P. Luo, Z. Lei, X. Luo, Prof. Dr. M. J. Koh, Prof. Dr. J. Wu
Department of Chemistry, National University of Singapore
3 Science Drive 3, Singapore 117543 (Singapore)
E-mail: chmkmj@nus.edu.sg
chmjie@nus.edu.sg

[**] A previous version of this manuscript has been deposited on a preprint server (https://doi.org/10.26434/chemrxiv-2023-gr02g).

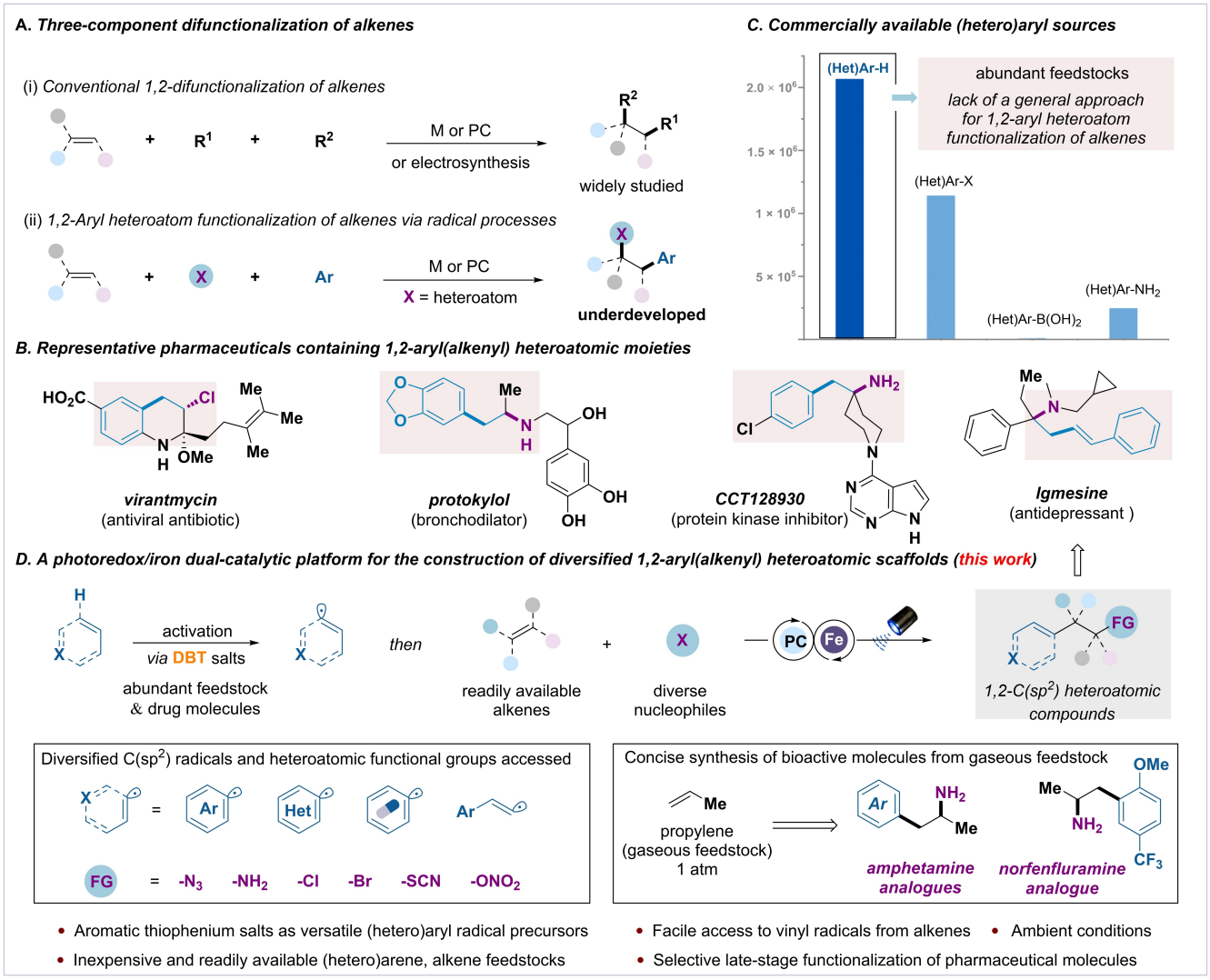

Figure 1. Photoredox/iron dual-catalyzed 1,2-aryl(alkenyl) heteroatom functionalization of alkenes. (A) Multi-component difunctionalization of alkenes for the construction of 1,2-aryl heteroatomic scaffolds. (B) Commercially available (hetero)aryl sources. The statistical data presented here are based on the number of commercially available compounds that are sourced from Reaxys, as of June 17, 2023. (C) Selected examples of bioactive molecules containing 1,2-aryl(alkenyl) heteroatomic moieties. (D) This work: A photoredox/iron dual catalysis for the construction of diverse 1,2-aryl(alkenyl) heteroatomic compounds from readily available (hetero)arenes, alkenes, and nucleophiles. M = transition-metal catalyst; PC = photocatalyst.

with excellent yield and site selectivity through electrophilic thianthrenation or a complementary Ir-catalyzed regioselective borylation followed by Cu-mediated thianthrenation for late-stage functionalization of complex bioactive molecules.[11,12b] During the course of compiling our manuscript, Ritter and co-workers extended the application of this strategy to three-component reactions, enabling aminoarylation of alkenes through a photoinduced copper-catalyzed pathway.[13a] Despite these recent advances,[13] the development of a unified synthetic platform capable of rapidly assembling a broad array of 1,2-aryl heteroatomic compounds from inexpensive and readily available aromatics and olefins remains an unmet challenge.

Over the past decade, iron (Fe) catalysis has gained significant attention in synthetic chemistry[14] by providing an attractive avenue for developing efficient methodologies to streamline the synthesis of complex organic molecules,[15] due to its cost-effectiveness, biocompatibility and environmental sustainability. While Fe-catalyzed multicomponent reactions offer unique opportunities beyond conventional transition-metal catalysis,[16] the application of inexpensive iron catalysts in three-component 1,2-aryl heteroatom functionalization of alkenes for constructing bioactive small molecules is still underdeveloped. In 2023, Leboeuf and coworkers reported a Fe-catalyzed two-step 1,2-aminoarylation of alkenes with arenes and hydroxylamines as the nitrogen source through a ring-opening strategy via an aziridinium intermediate.[16a] However, the scope of the reaction is limited to electron-deficient alkenes and electron-rich arenes. Therefore, there is still a need for more general ways to promote 1,2-aryl heteroatom functionalization of alkenes starting from commercially available aro-

matics and alkenes of diverse electronic/steric attributes. In this context, metallaphotoredox, the merger of photoredox and transition metal catalysis, has emerged as a promising strategy by offering a broader scope and greater generality.[17] Recently, Gaunt and co-workers demonstrated the use of a photoredox/iron catalytic approach for the vicinal arylchlorination of vinylboronic esters using diaryliodonium salts as the aryl radical source.[18] Building upon this concept, we report a mild, modular, and practical photoredox/iron dual catalytic system by leveraging aryl sulfonium salts as versatile building blocks, readily accessible from arenes in a regioselective manner. This system demonstrates a broad substrate scope, tolerating various (hetero)arenes, alkenes, and heteroatomic compounds, thereby providing a versatile platform for the synthesis of diverse 1,2-aryl heteroatomic pharmacophores (Figure 1D).

Additionally, this mild photoredox/iron dual-catalytic system offers a convenient method for the underdeveloped direct generation of 1,2-alkenyl heteroatomic compounds, an important class of medicinally relevant scaffolds that include homoallylamines (Figure 1B), using alkenes as the alkenyl radical precursors.

Results and Discussion

Reaction Optimization

The reaction development was initiated by using aryl dibenzothiophenium salt **4a** readily accessed from the corresponding arene as the model substrate for 1,2-arylazidation of alkenes with $TMSN_3$ under photoredox/iron dual-catalyzed conditions. Through extensive investigation of various bases, photocatalysts, iron catalysts, and solvents, the optimal conditions for the reaction were identified as follow: the combination of the photocatalyst *fac*-Ir(ppy)$_3$ (2 mol %), Fe(OTf)$_2$ (20 mol %), 4-picoline (2.5 equiv.) in MeCN (0.1 M) at room temperature under light irradiation with 456 nm blue light-emitting diode (LED) afforded arylethylazide product **4** in 84 % yield and complete regioselectivity (Table 1, entry 1). Notably, the residue dibenzo[b,d]thiophene (DBT) was recovered in 94 % yield and can be reused. When 4-picoline was replaced with other bases, the product yields decreased (entry 2). The choice of solvent was vital to this transformation, as evidenced by the low yield (0–60 %) obtained when using other solvents (entry 3, see Table S1 for details). Switching Fe(OTf)$_2$ to other iron catalysts also resulted in decreased yield of azidoarylation product **4** (Table 1, entry 4). Substituting the photocatalyst from *fac*-Ir(ppy)$_3$ (E^{red} [Ir(III*)/Ir(IV)] = −1.73 V *vs* SCE) to Ir(dFCF$_3$ppy)$_2$(dtbbpy)PF$_6$ (E^{red} [Ir(III*)/Ir(IV)] = −0.89 V *vs* SCE) or 4CzIPN (E^{red} [PC*/PC$^+$] = −1.01 V *vs* SCE)[19] led to no product formation, possibly because that their reduction potentials are not enough to reduce sulfonium salt **4a** (E^{red} = −1.1 V *vs* SCE)[12i] (entries 5 and 6). When NaN_3 was used as the nitrogen source instead of $TMSN_3$ and 4-picoline, the yield of desired product **4** was obtained in 69 % yield (entry 7). The yield of **4** descended when the TT salt **4b** was used (entry 8). In addition, control experiments showed that the absence of *fac*-Ir(ppy)$_3$, iron catalyst, 4-picoline or light resulted in no product formation, highlighting the necessity of these components in this reaction (entries 9–11).

Table 1: Evaluation of reaction conditions.

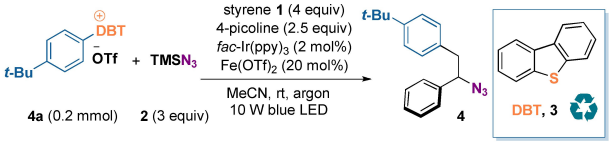

Entry	Deviation	Yield (%)[a]
1	**none**	**84 (82[b])**
2	pyridine or 4-*tert*-butylpyridine instead of 4-picoline	64/75
3	other solvents instead of MeCN	0-60
4	$Fe(OAc)_2$ or $FeCl_2$ instead of $Fe(OTf)_2$	57/70
5	$Ir(dFCF_3ppy)_2(dtbbpy)PF_6$ instead of *fac*-Ir(ppy)$_3$	0
6	4CzIPN instead of *fac*-Ir(ppy)$_3$	0
7	NaN_3 instead of $TMSN_3$ and 4-picoline	69
8	TT salts **4b** instead of **4a**	70
9	without *fac*-Ir(ppy)$_3$ or light	0
10	without $Fe(OTf)_2$	0
11	without 4-picoline	0

[a] Yields were determined by analysis of the crude ^{1}H NMR spectra using CH_2Br_2 as an internal standard. [b] Isolated yields. See Tables S1–S4 for details. TT salt **4*b*** = 5-(4-(*tert*-butyl)phenyl)-5*H*-thianthren-5-ium trifluoromethanesulfonate.

Substrate Scope

With the optimal reaction conditions in hand, we first explored the scope of (hetero)arenes in this three-component 1,2-arylazidation reaction. To our delight, this photoredox/iron co-catalyzed protocol is applicable to an extremely broad set of aromatic hydrocarbons and drug molecules, furnishing the desired products with exclusive regioselectivity across the board (Scheme 1). Arenes bearing a wide range of substituents, including electron-rich and electron-poor groups, in various substitution patterns (*ortho*-, *meta*-, and *para*-) afforded the desired azidoarylation products (**4**–**23**) in good to excellent yields. Heteroaromatics such as pyridine, quinoline, pyrrole, and thiophene were also well-tolerated (**24**–**29**). The mild photoredox/iron-catalyzed conditions coupled with the high site selectivity dictated by the synthesis of DBT salts[11] render this protocol a valuable tool for executing precise late-stage modifications of complex biologically relevant scaffolds and drug molecules. Numerous natural products and pharmaceuticals, including clofibrate, aniracetam, mexiletine, boscalid, nimesulide, estrone, diflunisal, chlorzoxazone, nefiracetam, fenofibrate, amiodarone, diclofenac amide, voltaren, ketanserin, famoxadone, benzbromarone, fenbufen, were well-tolerated, furnishing the corresponding late-stage-modified products (**30**–**46**) as single regioisomers in moderate to good yields. In general, the protocol exhibited excellent compatibility with numerous functional groups, including halogens (F, Cl, Br), silanes, esters, ethers, amides, sulfonamides, nitro ketones,

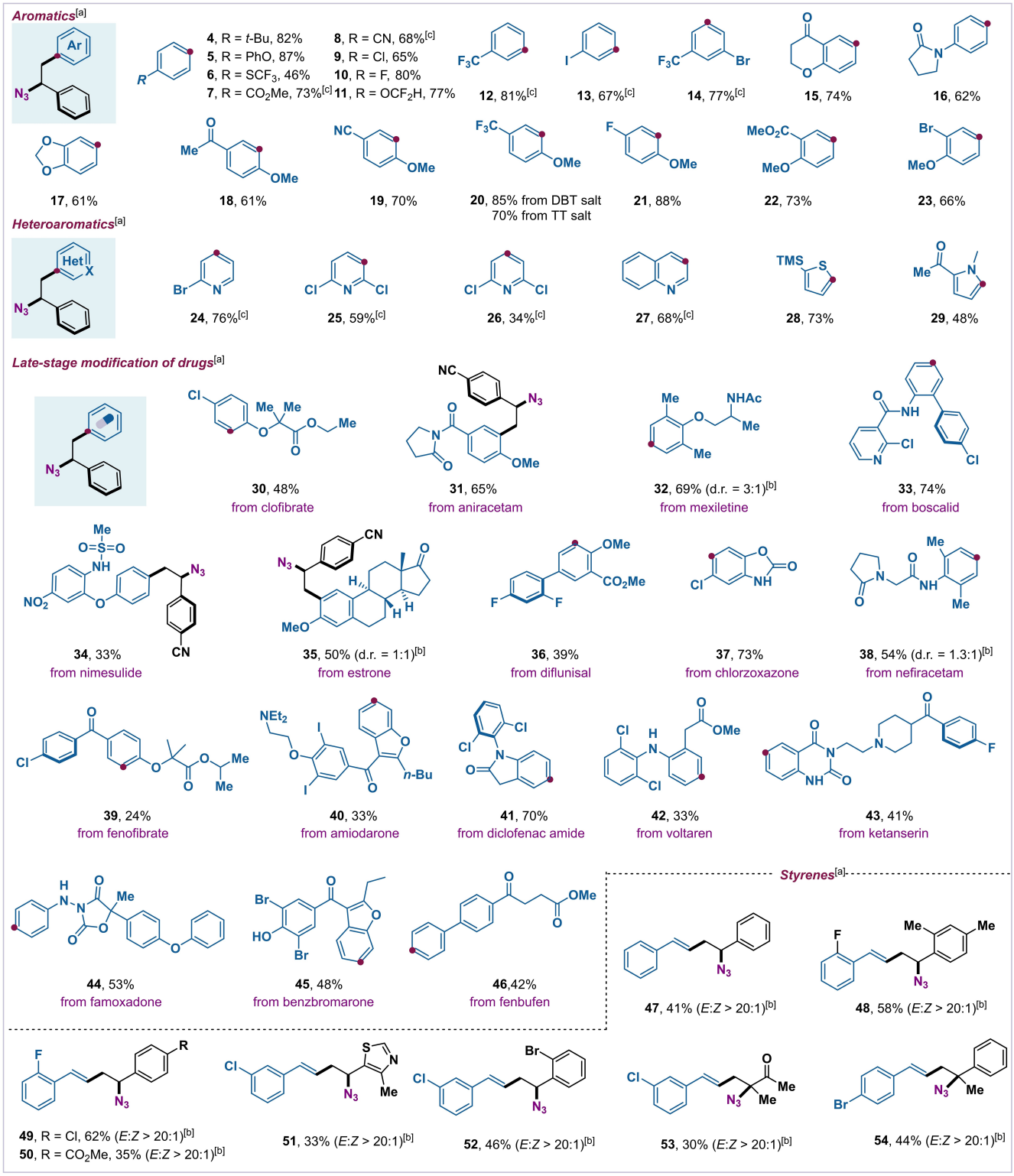

Scheme 1. Photoredox/iron dual catalysis for the synthesis of arylethylamines and homoallylamines. [a] All reactions were performed with DBT salts (0.2 mmol), olefins (4 equiv.), $TMSN_3$ (3 equiv.), 4-picoline (2.5 equiv.), *fac*-$Ir(ppy)_3$ (2 mol%), $Fe(OTf)_2$ (20 mol%) in MeCN (2.0 mL) under argon and 10 W blue LED irradiation. [b] Diastereomeric ratios (d.r.) or *E*/*Z* ratios were determined by analysis of the ^1H NMR spectra of the crude reaction mixtures [c] Arylthianthrenium salts (TT salts) were used.

nitriles, trifluoromethylthio-, difluoromethoxy-, and trifluoromethyl groups, as well as protic groups such as secondary amines and hydroxyl groups. Remarkably, this iron-catalyzed system exhibits exceptional compatibility

with aryl iodides affording the desired products in moderate yields (**13** and **40**) despite the labile nature of the Ar–I bond. Notably, in addition to aryl and heteroaryl cases, styrenyl DBT salts were viable substrates in this protocol, marking the first reported examples of direct 1,2-alkenyl azidation to generate products that can be further elaborated to valuable homoallylamines.[20] Styrenyl groups with different substituents could be installed to secure the desired products (**47–54**) in moderate yields and high regio- and stereoselectivity ($E:Z>20:1$).

To further assess the generality of this method, a broad range of readily accessible alkene substrates was investigated (Scheme 2). Activated alkenes such as 4-chlorostyrene, 2-vinylthiophene, vinylthiazole as well as vinyl ether were feasible to provide the corresponding products (**55–58**) in good to high yields. Cyclic disubstituted internal alkenes also effectively participated in this transformation, affording the desired azidoarylation product (**59–61**) in moderate yields with excellent diastereoselectivity (d.r. $>20:1$). Simple mono-substituted alkenes bearing sensitive functional groups, such as chloromethyl silane and bromide, were well-tolerated to deliver the corresponding products (**62**, **63**) in 66% and 57% yields, respectively. Furthermore, Michael acceptors could also be employed in the 1,2-aryl heteroatom functionalization to deliver the desired products (**64**, **65**). Moreover, 1,1-disubstituted alkenes, whether acyclic (**54**, **66**, **67**) or cyclic (**68–72)** with structures such as cyclobutane, piperidine, and adamantane rings, demonstrated favorable reactivity, delivering the tetrasubstituted azide products in moderate to good yields. Application of this method in the late-stage functionalization of complex natural products possessing an alkene moiety was also explored. Terminal alkenes found in the core structures of *L*(−)-carvone (**73**), nootkatone (**74**), vinclozolin (**76**), (+)-dihydrocarvone (**77**) smoothly underwent the 1,2-azidoarylation.

Importantly, by simply replacing the azide with other nucleophiles, a diverse library of 1,2-aryl heteroatomic skeletons can be rapidly constructed through photoredox/iron dual catalysis. This versatile protocol enables the efficient synthesis of 1,2-arylsulfenylated products (**78–79**), 1,2-arylnitrooxylated product (**80**), 1,2-arylbrominated products (**81–82**), and 1,2-arylchlorinated products (**83–86**), offering a powerful platform towards the preparation of diverse 1,2-aryl heteroatomic compounds.

Further Synthetic Applications

The synthetic utility of this method was further demonstrated in several transformations of the multifunctional azido products (Scheme 3). Firstly, the 1,2-arylazidation reaction can be easily scaled up to gram quantities, emphasizing its practical utility (Scheme 3A). Reduction of azido-modified diclofenac amide **42** afforded primary amine **87** in good yield. Copper-catalyzed click reaction of diclofenac amide analogue **42** with acetylene gas provided triazole **88** in 56% yield. Cycloaddition of chlorzoxazone derivative **38** with pentane-2,4-dione resulted in the formation of triazole **89**. Additionally, azide **38** can be further converted into phosphorimidate **90** in 92% yield under mild reducing conditions. The bioconjugation of azides (**38** and **42**) with pharmaceuticals and natural product moieties, such as mestranol, mestranol, fenbufen derivatives, via click chemistry provided feasible access to adducts **91–93** in good yields, suggesting the potential applications in the preparation of antibody-drug conjugates and biomolecule labeling. Phenethylamines, including amphetamine and its derivatives, are naturally occurring compounds with promising biological activities for central nervous system treatments, making them appealing in drug development. We then turned our attention to the synthesis of β-phenethylamine drugs from feedstock chemicals (Scheme 3B). The tandem azidation and reduction using commercially available aromatics with propylene enabled the rapid synthesis of norfenfluramine and amphetamine analogues (**94–97** and **101**). Moreover, this protocol was successfully employed to construct the key synthetic intermediate for bronchial drug protokylol[3c,21] (**98**) and the adenosine triphosphate (ATP)-competitive protein kinase B (Akt) inhibitor CCT128930 (**102**).[3b]

Mechanistic Studies

A series of control experiments and spectroscopic investigations were conducted to elucidate the reaction mechanisms (Scheme 4). In the absence of Fe catalysts, no product **4a** or Ritter-type amination product **104** were detected, ruling out the possibility of a radical-polar crossover and subsequent carbocation trapping pathway (Scheme 4A, i). When iron(II)-azide complex **105**,[22] which was prepared from $FeSO_4{\cdot}H_2O$, 4-picoline and NaN_3 in water,[23] was subjected to the standard reaction conditions with DBT salt **4a** and styrene, the desired product **4** was obtained in 79% NMR yield (Scheme 4A, ii). This result highlights the importance of the iron catalyst in the azide transfer process; however, further investigation is necessary to fully comprehend its role in these processes. Furthermore, the oxidation potential of Fe(II) complex **105** at $E^{ox}=0.53$ V *vs* SCE, was measured by cyclic voltammetry. This result demonstrated that the oxidized Ir(IV) catalytic species ($E_{1/2}{}^{ox}=$[Ir(IV)/Ir(III)]$=0.77$ V *vs* SCE) could be potentially reduced by a putative iron(II)-azide species to generate iron(III) intermediate and Ir(III) species. Additionally, a radical clock experiment using cyclopropyl styrene **106** under the standard conditions led to the formation of ring-opened product **108** in 45% isolated yield. This result confirms the generation of aryl radical from DBT salt and its subsequent addition to styrene, which formed radical intermediate **107** through the radical ring opening of the cyclopropyl group (Scheme 4B). To further establish the light-dependency of this reaction, an intermittent illumination experiment was performed, and the results demonstrated a clear correlation between irradiation and productivity (Scheme 4C). Importantly, no product formation was observed during the dark phase, eliminating the possibility of any thermal processes and firmly establishing that the reaction is specifically triggered by light. This observation also underscores the

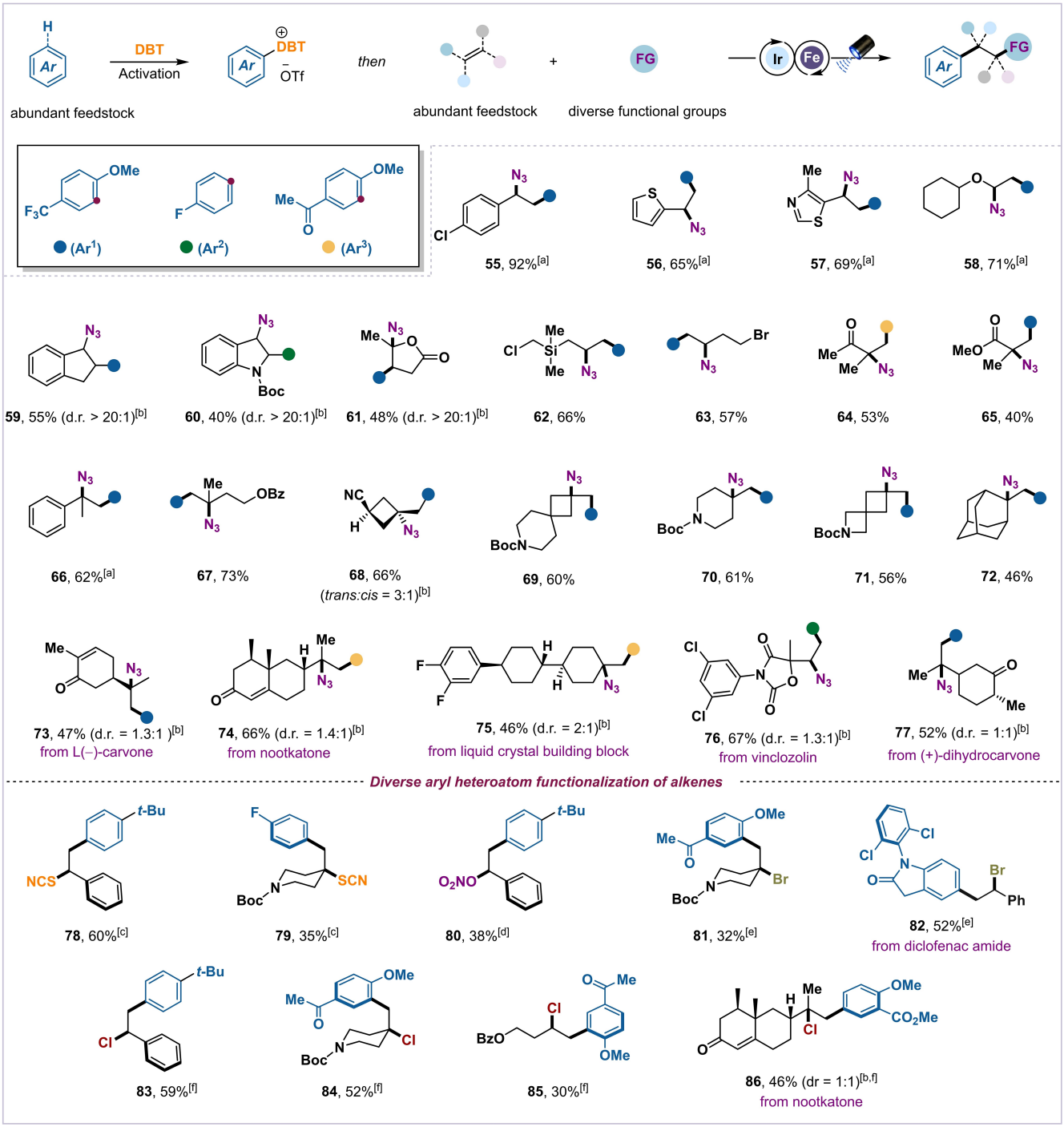

Scheme 2. Diverse synthesis 1,2-aryl heteroatomic compounds. All reactions were performed with DBT salt (0.2 mmol), olefins (4 equiv.), NaN_3 (3 equiv.), *fac*-Ir(ppy)$_3$ (2 mol%), Fe(OTf)$_2$ (20 mol%) in MeCN (2.0 mL) under argon and 10 W blue LED irradiation, unless otherwise indicated. [a] $TMSN_3$ (3 equiv.), 4-picoline (2.5 equiv.) instead of NaN_3. [b] Diastereomeric ratios (d.r.) were determined by the analysis of ^{1}H NMR spectra of the crude reaction mixtures. [c] 3.0 equiv. of KSCN was used; [d] 3.0 equiv. of *n*-Bu_4NNO_3 was used; [e] 3.0 equiv. of *n*-Bu_4NBr was used. [f] 3.0 equiv. of *n*-Bu_4NCl was used.

crucial role of photocatalyst *fac*-Ir(ppy)$_3$ in facilitating the reaction. Furthermore, the measured quantum yield (Φ) value ($\Phi = 4\times10^{-2}$, see the Supporting Information for details) supports a closed photocatalytic cycle instead of a chain radical process. Additionally, Stern–Volmer luminescence quenching studies showed that DBT salt **4a** quenched the excited state of *fac*-Ir(ppy)$_3$ dramatically more than other quenchers, providing evidence for the preferential interaction between the DBT salt and the photo-excited catalytic species (Scheme 4D). Based on the experimental findings and previous literatures,[12i,l,16i,18] a tentative mechanism is proposed as depicted in Scheme 4E. Under light

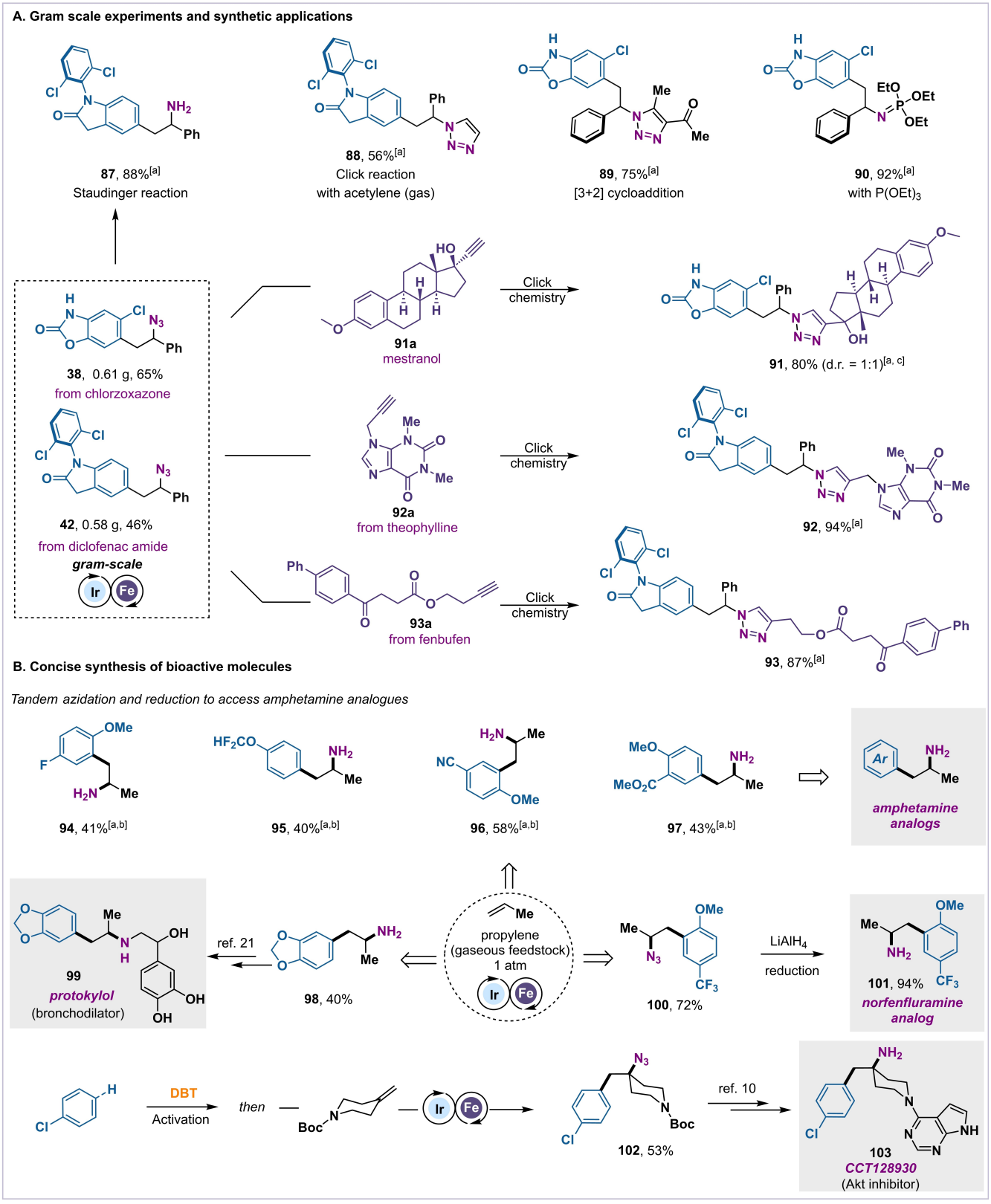

Scheme 3. Further synthetic applications. [a] For detailed reaction conditions, please refer to the Supporting Information. [b] Two-step overall yields were indicated. [c] Diastereomeric ratio (d.r.) was determined by the analysis of ^{1}H NMR spectra of the crude reaction mixture.

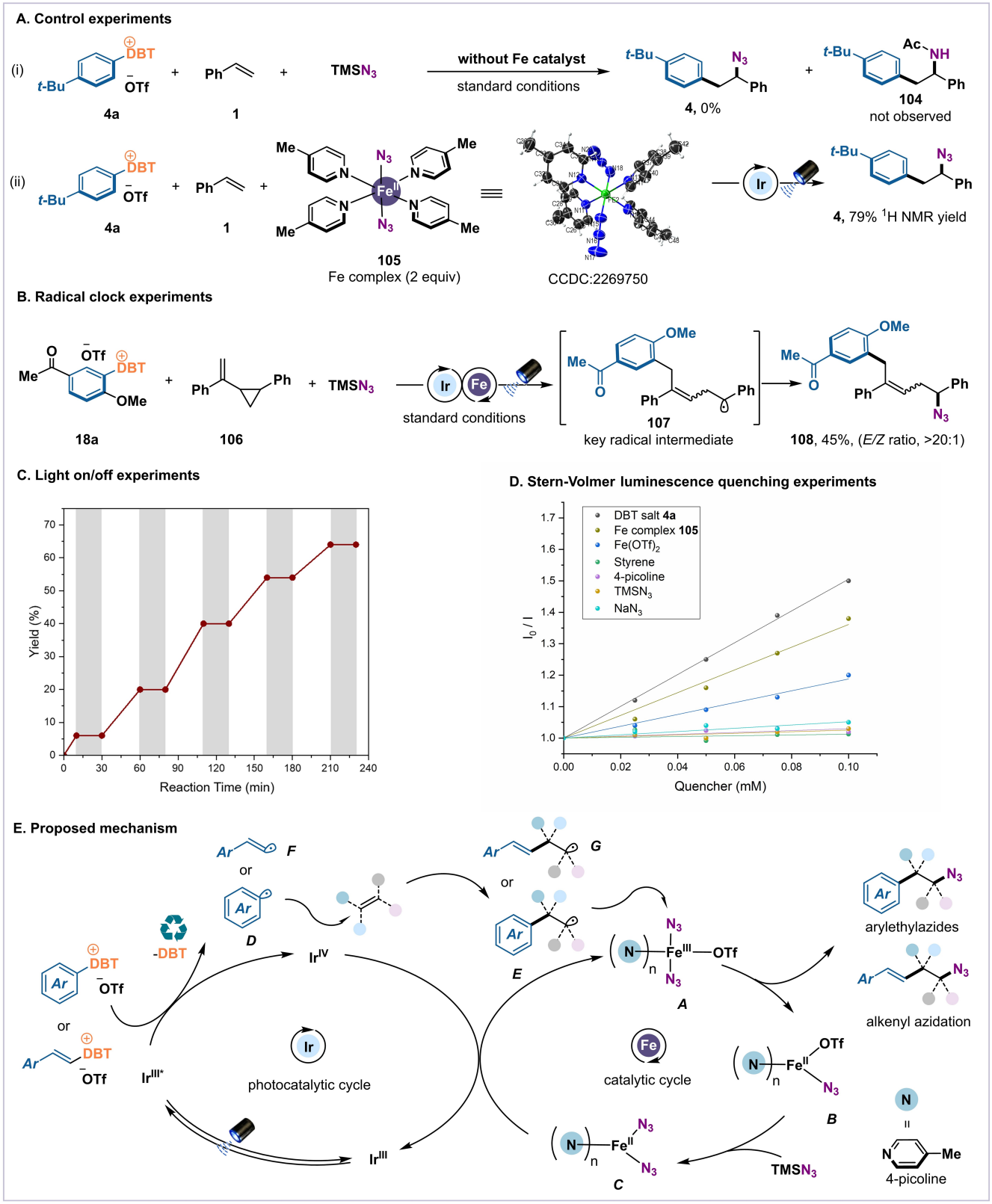

Scheme 4. Proposed mechanisms with supporting evidence.

irradiation, the excited Ir(III)* catalyst ($E_{1/2}^{red}$ [Ir(III*)/Ir(IV)] = −1.73 V *vs* SCE)[24] reduces the DBT salt (**4a**, E^{red} = −1.1 V *vs* SCE), generating the corresponding aryl radical **D** or alkenyl radical **F** and releasing DBT. The aryl/

alkenyl radical then exclusively adds to the alkene selectively at a position that generates the stabilized alkyl radical **E** or **G**. Although the precise details of the iron catalytic mechanism are not fully understood at this stage, it is hypothesized that an in situ generated iron(II)-azide species **C** (analogous to **105**), formed from the combination of $Fe(OTf)_2$, 4-picoline and $TMSN_3$ in MeCN, reduces the oxidized state Ir(IV) catalyst ($E_{1/2}^{ox}=[Ir(IV)/Ir(III)]=0.77$ V *vs* SCE), leading to the formation of iron(III) intermediate **A** and regeneration of the Ir(III) catalyst to complete the photocatalytic cycle. Finally, radical intermediate **E** or **G** can be trapped by **A** to deliver iron(II) complex **B** and the desired coupling products.

Conclusion

In summary, we have developed a mild, modular, and practical photoredox/iron dual-catalytic system for the direct access of diverse medicinally valuable 1,2-aryl(alkenyl) heteroatomic compounds from readily available starting materials such as (hetero)arenes, alkenes, and heteroatomic compounds. This methodology offers a broad substrate scope and is applicable to late-stage functionalization of complex bioactive molecules in a highly selective fashion, making it a valuable tool in drug discovery and development. The scalability of this protocol and the successful rapid synthesis of a range of bioactive molecules further underscore its practicality and synthetic utility.

Acknowledgements

We are grateful for the financial support provided by the Ministry of Education (MOE) of Singapore (MOE-T2EP10120-0014), Pfizer (A-0004153-00-00), National Research Foundation, the Prime Minister's Office of Singapore under its NRF-CRP Programme (award no. NRF-CRP25-2020RS-0002).

Conflict of Interest

The authors declare no conflict of interest.

Data Availability Statement

The data that support the findings of this study are available in the supplementary material of this article.

Keywords: Difunctionalization · Iron Catalyst · Late-Stage Functionalization · Metallaphotoredox · Multicomponent

[1] For selected reviews, see: a) L. M. Wickham, R. Giri, *Acc. Chem. Res.* **2021**, *54*, 3415–3437; b) S. Zhu, X. Zhao, H. Li, L. L. Chu, *Chem. Soc. Rev.* **2021**, *50*, 10836–10856; c) X. Chen, F. Xiao, W.-M. He, *Org. Chem. Front.* **2021**, *8*, 5206–5228; d) Z. L. Zou, W. Zhang, Y. Wang, Y. Pan, *Org. Chem. Front.* **2021**, *8*, 2786–2798; e) M. J. Cabrera-Afonso, A. Sookezian, S. O. Badir, M. El Khatib, G. A. Molander, *Chem. Sci.* **2021**, *12*, 9189–9195; f) J. S. Zhang, L. Liu, T. Chen, L. B. Han, *Chem. Asian J.* **2018**, *13*, 2277–2291; g) G. Yin, X. Mu, G. Liu, *Acc. Chem. Res.* **2016**, *49*, 2413–2423 For selected recent seminal work, see: h) H. Y. Tu, F. Wang, L. Huo, Y. Li, S. Zhu, X. Zhao, H. Li, F. L. Qing, L. L. Chu, *J. Am. Chem. Soc.* **2020**, *142*, 9604–9611; i) L. Guo, M. Yuan, Y. Zhang, F. Wang, S. Zhu, O. Gutierrez, L. L. Chu, *J. Am. Chem. Soc.* **2020**, *142*, 20390–20399; j) S. O. Badir, G. A. Molander, *Chem* **2020**, *6*, 1327–1339; k) X. Zhao, H. Y. Tu, L. Guo, S. Zhu, F. L. Qing, L. L. Chu, *Nat. Commun.* **2018**, *9*, 3488.

[2] For selected recent seminal work, see: a) W. Lee, Y. Koo, H. Jung, S. Chang, S. Hong, *Nat. Chem.* **2023**, *15*, 1091–1099; b) M. Kim, Y. Koo, S. Hong, *Acc. Chem. Res.* **2022**, *55*, 3043–3056; c) H. Im, W. Choi, S. Hong, *Angew. Chem. Int. Ed.* **2020**, *59*, 17511–17516; d) Y. Moon, W. Lee, S. Hong, *J. Am. Chem. Soc.* **2020**, *142*, 12420–12429; e) Y. Moon, B. Park, I. Kim, G. Kang, S. Shin, D. Kang, M.-H. Baik, S. Hong, *Nat. Commun.* **2019**, *10*, 4117; f) H.-B. Yang, S. R. Pathipati, N. Selander, *ACS Catal.* **2017**, *7*, 8441–8445; g) D. Wang, L. Wu, F. Wang, X. Wan, P. Chen, Z. Lin, G. Liu, *J. Am. Chem. Soc.* **2017**, *139*, 6811–6814; h) Z. Liu, Y. Wang, Z. Wang, T. Zeng, P. Liu, K. M. Engle, *J. Am. Chem. Soc.* **2017**, *139*, 11261–11270; i) M. Schulze, *Synth. Commun.* **2010**, *40*, 1461–1476; j) G. Z. Zhang, L. Cao, Y. Z. Wang, L. M. Zhang, *J. Am. Chem. Soc.* **2010**, *132*, 1474–1475; k) W. E. Brenzovich Jr., D. Benitez, A. D. Lackner, H. P. Shunatona, E. Tkatchouk, W. A. Goddard III, F. D. Toste, *Angew. Chem. Int. Ed.* **2010**, *49*, 5519–5522.

[3] a) G. W. Gribble, *Mar. Drugs* **2015**, *13*, 4044–4136; b) J. C. John, G. D. Thomas, D. Alastair, M. Tatiana, G. R. Martin, A. G. Wynne, K. H. Lisa, T. Kevin, R. Ruth, I. R. Florence, V. Marcel W Paul, D. G. Michelle, C. Ian, *J. Med. Chem.* **2008**, *51*, 2147–2157; c) B. Waldeck, *Eur. J. Pharmacol.* **2002**, *445*, 1–12; d) H. C. Akunne, K. T. Zoski, S. Z. Whetzel, J. J. Cordon, R. M. Brandon, F. Roman, T. A. Pugsley, *Neuropharmacology* **2001**, *41*, 138–149; e) G. W. Gribble, *J. Nat. Prod.* **1992**, *55*, 1353–1395.

[4] a) K. Semba, Y. Ohtagaki, Y. Nakao, *Tetrahedron Lett.* **2021**, *72*, 153059; b) Z. Liu, X. Li, T. Zeng, K. M. Engle, *ACS Catal.* **2019**, *9*, 3260–3265; c) Z. Liu, H. Q. Ni, T. Zeng, K. M. Engle, *J. Am. Chem. Soc.* **2018**, *140*, 3223–3227.

[5] a) K. Dipannita, A. D. Satterfield, M. S. Sanford, *J. Am. Chem. Soc.* **2010**, *132*, 8419–8427; b) K. Dipannita, M. S. Sanford, *J. Am. Chem. Soc.* **2008**, *130*, 2150–2151.

[6] a) S. Zhang, C. Wang, X. Ye, X. Shi, *Angew. Chem. Int. Ed.* **2020**, *59*, 20470–20474; b) W. E. Brenzovich, J. J.-F. Brazeau, F. D. Toste, *Org. Lett.* **2010**, *12*, 4728–4731; c) A. D. Melhado, W. E. Brenzovich, J. A. D. Lackner, F. D. Toste, *J. Am. Chem. Soc.* **2010**, *132*, 8885–8887.

[7] Z. Q. Li, Y. Cao, T. Kang, K. M. Engle, *J. Am. Chem. Soc.* **2022**, *144*, 7189–7197.

[8] a) D. M. Schultz, J. P. Wolfe, *Synthesis* **2012**, *44*, 351–361; b) E. Tkatchouk, N. P. Mankad, D. Benitez, W. A. Goddard III, F. D. Toste, *J. Am. Chem. Soc.* **2011**, *133*, 14293–14300.

[9] a) S. Kindt, K. Wicht, M. R. Heinrich, *Org. Lett.* **2015**, *17*, 6122–6125; b) D. Prasad Hari, T. Hering, B. König, *Angew. Chem. Int. Ed.* **2014**, *53*, 725–728; c) S. B. Gabriele Fumagalli, F. Michael, *Org. Lett.* **2013**, *15*, 4398–4401.

[10] A. Bunescu, Y. Abdelhamid, M. J. Gaunt, *Nature* **2021**, *598*, 597–603.

[11] F. Berger, M. B. Plutschack, J. Riegger, W. Yu, S. Speicher, M. Ho, N. Frank, T. Ritter, *Nature* **2019**, *567*, 223–228.

[12] a) A. Dewanji, L. van Dalsen, J. A. Rossi-Ashton, E. Gasson, G. E. M. Crisenza, D. J. Procter, *Nat. Chem.* **2023**, *15*, 43–52; b) X. Y. Chen, Y. N. Li, Y. Wu, J. Bai, Y. Guo, P Wang, *J. Am.*

Chem. Soc. **2023**, *145*, 10431–10440; c) X.-Y. Chen, Y. Wu, P. Wang, *Synthesis* **2022**, *54*, 3928–3940; d) B. Lansbergen, P. Granatino, T. Ritter, *J. Am. Chem. Soc.* **2021**, *143*, 7909–7914; e) Y.-L. Zhang, G.-H. Wang, Y. Wu, C.-Y. Zhu, P. Wang, *Org. Lett.* **2021**, *23*, 8522–8526; f) J. Wu, Z. Wang, X.-Y. Chen, Y. Wu, D. Wang, Q. Peng, P. Wang, *Sci. China Chem.* **2020**, *63*, 336–340; g) P. Xu, D. Zhao, F. Berger, A. Hamad, J. Rickmeier, R. Petzold, M. Kondratiuk, K. Bohdan, T. Ritter, *Angew. Chem. Int. Ed.* **2020**, *59*, 1956–1960; h) J. Li, J. Chen, R. Sang, W. S. Ham, M. B. Plutschack, F. Berger, S. Chabbra, A. Schnegg, C. Genicot, T. Ritter, *Nat. Chem.* **2020**, *12*, 56–62; i) M. H. Aukland, M. Šiaučiulis, A. West, G. J. P. Perry, D. J. Procter, *Nat. Catal.* **2020**, *3*, 163–169; j) F. Ye, F. Berger, H. Jia, J. Ford, A. Wortman, J. Borgel, C. Genicot, T. Ritter, *Angew. Chem. Int. Ed.* **2019**, *58*, 14615–14619; k) P. S. Engl, A. P. Haring, F. Berger, G. Berger, A. Perez-Bitrian, T. Ritter, *J. Am. Chem. Soc.* **2019**, *141*, 13346–13351; l) R. C. Sang, S. E. Korkis, W. Q. Su, F. Ye, P. S. Engl, F. Berger, T. Ritter, *Angew. Chem. Int. Ed.* **2019**, *58*, 16161–16166.

[13] a) Y. Cai, S. Chatterjee, T. Ritter, *J. Am. Chem. Soc.* **2023**, *145*, 13542–13548; b) Y. Cai, T. Ritter, *Angew. Chem. Int. Ed.* **2022**, *61*, e202209882; c) D. E. Holst, C. Dorval, C. K. Winter, I. A. Guzer, Z. K. Wickens, *J. Am. Chem. Soc.* **2023**, *145*, 8299–8307.

[14] For selected reviews: a) Y. Liu, K.-P. Shing, V. K.-Y. Lo, C.-M. Che, *ACS Catal.* **2023**, *13*, 1103–1124; b) N. J. Bakas, M. L. Neidig, *ACS Catal.* **2021**, *11*, 8493–8503; c) D. Wei, C. Darcel, *Chem. Rev.* **2019**, *119*, 2550–2610.

[15] a) Q. Wang, Q. Sun, Y. Jiang, H. Zhang, L. Yu, C. Tian, G. Chen, M. J. Koh, *Nat. Synth.* **2022**, *1*, 235–244; b) X. Yu, H. Zheng, H. Zhao, B. C. Lee, M. J. Koh, *Angew. Chem. Int. Ed.* **2021**, *60*, 2104–2109; c) X. Yu, H. Zhao, S. Xi, Z. Chen, X. Wang, L. Wang, L. Q. H. Lin, K. P. Loh, M. J. Koh, *Nat. Catal.* **2020**, *3*, 585–592; d) A. Fürstner, *ACS Cent. Sci.* **2016**, *2*, 778–789; e) C. Bolm, J. Legros, J. L. Paih, L. Zani, *Chem. Rev.* **2004**, *104*, 6217–6254.

[16] a) V. Pozhydaiev, M. Vayer, C. Fave, J. Moran, D. Leboeuf, *Angew. Chem. Int. Ed.* **2023**, *62*, e202215257; b) M. Zhang, J. Zhang, Q. Li, Y. Shi, *Nat. Commun.* **2022**, *13*, 7880; c) K.-J. Bian, S.-C. Kao, D. Nemoto Jr, X.-W. Chen, J. G. West, *Nat. Commun.* **2022**, *13*, 7881; d) L. Liu, M. C. Aguilera, W. Lee, C. R. Youshaw, M. L. Neidig, O. Gutierrez, *Science* **2021**, *374*, 432–439; e) D. Lv, Q. Sun, H. Zhou, L. Ge, Y. Qu, T. Li, X. Ma, Y. Li, H. L. Bao, *Angew. Chem. Int. Ed.* **2021**, *60*, 12455–12460; f) R. Xu, C. Cai, *Org. Chem. Front.* **2020**, *7*, 318–323; g) S. Makai, E. Falk, B. Morandi, *J. Am. Chem. Soc.* **2020**, *142*, 21548–21555; h) L. Liu, W. Lee, C. R. Youshaw, M. Yuan, M. B. Geherty, P. Y. Zavalij, O. Gutierrez, *Chem. Sci.* **2020**, *11*, 8301–8305; i) L. Ge, H. Zhou, M.-F. Chiou, H. Jiang, W. Jian, C. Ye, X. Li, X. Zhu, H. Xiong, Y. Li, L. Song, X. Zhang, H. Bao, *Nat. Catal.* **2020**, *4*, 28–35; j) X.-H. Ouyang, Y. Li, R.-J. Song, M. Hu, S. Luo, J.-H. Li, *Sci. Adv.* **2019**, *5*, eaav9839; k) T. Shen, Y. Yuan, S. Song, N. Jiao, *Chem. Commun.* **2014**, *50*, 4115–4118.

[17] A. Y. Chan, I. B. Perry, N. B. Bissonnette, B. F. Buksh, G. A. Edwards, L. I. Frye, O. L. Garry, M. N. Lavagnino, B. X. Li, Y. Liang, E. Mao, A. Millet, J. V. Oakley, N. L. Reed, H. A. Sakai, C. P. Seath, D. W. C. MacMillan, *Chem. Rev.* **2022**, *122*, 1485–1542.

[18] B. Li, A. Bunescu, M. J. Gaunt, *Chem* **2023**, *9*, 216–226.

[19] T. Y. Shang, L. H. Lu, Z. Cao, Y. Liu, W. M. He, B. Yu, *Chem. Commun.* **2019**, *55*, 5408–5419.

[20] C. O. Puentes, V. Kouznetsov, *J. Heterocycl. Chem.* **2002**, *39*, 595.

[21] J. H. Biel, E. G. Schwarz, E. P. Sprengeler, H. A. Leiser, H. L. Friedman, *J. Am. Chem. Soc.* **1954**, *76*, 3149–3153.

[22] Deposition number 2269750 (for **105**) contains the supplementary crystallographic data for this paper. These data are provided free of charge by the joint Cambridge Crystallographic Data Centre and Fachinformationszentrum Karlsruhe Access Structures service.

[23] M. A. M. Abu-Youssef, V. Langer, D. Luneau, E. Shams, M. A. S. Goher, L. Öhrström, *Eur. J. Inorg. Chem.* **2007**, 112–118.

[24] C. K. Prier, D. A. Rankic, D. W. MacMillan, *Chem. Rev.* **2013**, *113*, 5322–5363.

Manuscript received: July 31, 2023
Accepted manuscript online: September 12, 2023
Version of record online: ■■, ■■

Research Articles

Dual Catalysis

W. Zhang, T. Liu, H. T. Ang, P. Luo, Z. Lei, X. Luo, M. J. Koh,* J. Wu* — **e202310978**

Modular and Practical 1,2-Aryl(Alkenyl) Heteroatom Functionalization of Alkenes through Iron/Photoredox Dual Catalysis

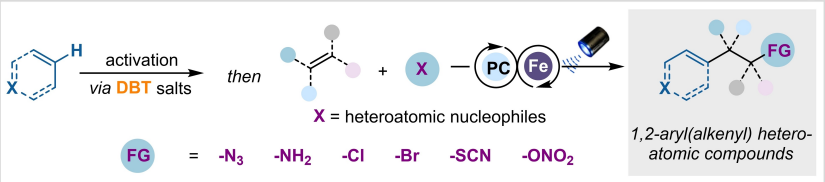

A practical photoredox/iron dual catalytic system has been developed for efficient synthesis of 1,2-aryl(alkenyl) heteroatomic cores with high site selectivity. The excellent functional group compatibility, scalability, use of readily available starting materials, and application to late-stage functionalization underscore the potential protocol's utility in medicinal chemistry and pharmaceutical research.